Domain Interactions between Streptokinase and Human Plasminogen†

Jeffrey A. Loy,‡,§ Xinli Lin,‡ Monica Schenone,|| Francis J. Castellino,|| Xuejun C. Zhang,⊥ and Jordan Tang*,‡,§

Protein Studies Program and Crystallography Research Program, Oklahoma Medical Research Foundation, 825 Northeast 13th Street, and Department of Biochemistry and Molecular Biology, University of Oklahoma Health Sciences Center, 940 Stanton L. Young Street, Oklahoma City, Oklahoma 73104, and Department of Chemistry and Biochemistry, University of Notre Dame, Notre Dame, Indiana 46556

Received June 22, 2001; Revised Manuscript Received October 2, 2001

ABSTRACT: Plasmin (Pm), the main fibrinolytic protease in the plasma, is derived from its zymogen plasminogen (Plg) by cleavage of a peptide bond at Arg^{561}−Val^{562}. Streptokinase (SK), a widely used thrombolytic agent, is an efficient activator of human Plg. Both are multiple-domain proteins that form a tight 1:1 complex. The Plg moiety gains catalytic activity, without peptide bond cleavage, allowing the complex to activate other Plg molecules to Pm by conventional proteolysis. We report here studies on the interactions between individual domains of the two proteins and their roles in Plg activation. Individually, all three SK domains activated native Plg. While the SK α domain was the most active, its activity was uniquely dependent on the presence of Pm. The SK γ domain also induced the formation of an active site in Plg_{R561A}, a mutant that resists proteolytic activation. The α and γ domains together yielded synergistic activity, both in Plg activation and in Plg_{R561A} active site formation. However, the synergistic activity of the latter was dependent on the correct N-terminal isoleucine in the α domain. Binding studies using surface plasmon resonance indicated that all three domains of SK interact with the Plg catalytic domain and that the β domain additionally interacts with Plg kringle 5. These results suggest mechanistic steps in SK-mediated Plg activation. In the case of free Plg, complex formation is initiated by the rapid and obligatory interaction between the SK β domain and Plg kringle 5. After binding of all SK domains to the catalytic domain of Plg, the SK α and γ domains cooperatively induce the formation of an active site within the Plg moiety of the activator complex. Substrate Plg is then recognized by the activator complex through interactions predominately mediated by the SK α domain.

Dissolution of fibrin clots is the central strategy in the short-term clinical treatment of blood clotting disorders, especially in acute myocardial infarction. Blood clot lysis is initiated by the activation of plasminogen (Plg)[1] to plasmin (Pm), which then degrades the fibrin clot into soluble peptides. Human Plg is a 92 kDa glycoprotein containing seven structural domains (Figure 1): a N-terminal peptide (NTP), five kringle domains (K1 through K5, respectively), and a serine protease catalytic domain (*1*). Native Plg contains a glutamic acid as its N-terminal residue and is referred to as Glu-Plg. However, after activation into Pm, the NTP is removed by cleavage of the Lys^{77}−Lys^{78} peptide bond (*2*). Incubation of Glu-Plg with Pm also results in removal of the NTP, generating Lys-Plg (*3*). The Plg kringles contain lysine-binding sites (*4*−*9*) that interact with lysine residues of other proteins, including fibrin (*1*, *10*−*13*), and with lysine analogues, such as ϵ-aminocaproic acid (EACA) (*4*, *14*, *15*). The Plg catalytic domain, devoid of any kringles, is referred to as μPlg, while the catalytic domain together with kringle 5 is called mini-Plg (Figure 1) (*1*, *16*). Both of these truncated forms of Plg are capable of being activated by Plg activators (*16*−*18*) and thus are models for the study of Plg activation mechanisms.

The conformation of Plg is mediated through the lysine-binding sites in its kringles. As a result of interactions between the NTP and the lysine-binding site of kringle 5, free Glu-Plg adopts a closed compact spiral conformation (*19*−*21*), which is favored in the presence of physiological levels of chloride ions (*22*−*24*). Pm-catalyzed conversion to Lys-Plg is accompanied by a large conformational change to an extended conformation, characterized by an accelerated rate of activation (*2*, *25*, *26*). Reduction in the levels of Cl^- or interaction between the lysine-binding site of one or more

† This work was supported by National Institutes of Health Grant HL-60626 (to X.C.Z.) and American Heart Association, Heartland Affiliate, Fellowship Award 0020419Z (to J.A.L.).

* To whom correspondence should be addressed. Phone: (405) 271-7291. Fax: (405) 271-7249. E-mail: jordan-tang@omrf.ouhsc.edu.

‡ Protein Studies Program, Oklahoma Medical Research Foundation.

§ Department of Biochemistry and Molecular Biology, University of Oklahoma Health Sciences Center.

|| Department of Chemistry and Biochemistry, University of Notre Dame.

⊥ Crystallography Research Program, Oklahoma Medical Research Foundation.

[1] Abbreviations: Plg, human plasminogen; Plg_{R561A}, Plg with residue 561 mutated from an arginine to an alanine; Pm, human plasmin; μPlg, human microplasminogen; μPlg_{S741A}, μPlg with residue 741 mutated from a serine to an alanine; μPm, human microplasmin; mini-Plg, human miniplasminogen; mini-Plg_{S741A}, mini-Plg with residue 741 mutated from a serine to an alanine; NTP, human plasminogen N-terminal peptide; K1 through K5, human plasminogen kringles 1 through 5, respectively; SK, streptokinase; SKα, SK α domain; SKβ, SK β domain; SKγ, SK γ domain; ΔM, deletion of N-terminal methionine; EACA, ϵ-aminocaproic acid; EDTA, ethylenediaminetetraacetic acid; SDS, sodium dodecyl sulfate; PAGE, polyacrylamide gel electrophoresis; *N*-*p*-tosyl-Gly-Pro-Lys-*p*NA, *N*-*p*-tosylglycylprolyllysine *p*-nitroanilide; ϵ_{280}, molar extinction coefficient at 280 nm; A_{406}, absorbance at 406 nm; AU, absorbance units; RU, resonance units; K_d, equilibrium dissociation constant; k_{on}, association rate constant; k_{off}, dissociation rate constant.

10.1021/bi011309d CCC: $20.00 © 2001 American Chemical Society
Published on Web 11/07/2001

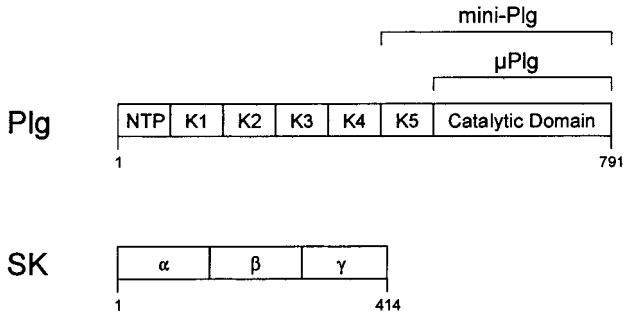

FIGURE 1: Domain organization of Plg and SK. Plg contains 791 amino acids and is organized into seven domains: a N-terminal peptide (NTP), five kringles (K1 through K5, respectively), and a catalytic domain. The domains comprising μPlg and mini-Plg are indicated. SK contains 414 amino acids and is organized into three domains, designated α, β, and γ.

of the kringles and fibrin, lysine, or lysine analogues also induces a conformational transition to an extended conformation (*22*−*24*, *27*−*31*).

Plg is activated into Pm by cleavage of the Arg^{561}−Val^{562} peptide bond, which is directly catalyzed by the proteases tissue plasminogen activator and urokinase. The mechanism of activation is essentially the same as that for other serine protease zymogens. After cleavage of the activation bond, the newly formed N-terminus of Val^{562} inserts inwardly to form a salt linkage with Asp^{740}, which triggers the formation of a catalytically competent active site (*32*). The streptococcal protein SK is not a protease itself and cannot directly cleave the Plg activation bond. However, SK forms a tight-binding stoichiometric complex with Plg, and it is this activator complex that is responsible for the activation of other Plg molecules into Pm (*33*−*36*). The catalytic apparatus of the activator complex is the active site of Plg (*33*, *34*, *37*, *38*). After complex formation, Plg within the complex is rapidly converted to Pm (*39*). Although Pm alone cannot activate Plg, the complex of SK−Pm, like the SK−Plg complex, is a Plg activator (*40*). The mechanism of Plg activation by SK requires at least three different SK properties: (i) high-affinity binding to Plg resulting in complex formation, (ii) inducing a nonproteolytic conformational change resulting in the formation of a Plg active site, and (iii) providing affinity of the activator complex for substrate Plg. The crystal structure of SK complexed with the Pm catalytic domain (μPm) illustrates that SK consists of three independently folding structural domains, α, β, and γ (Figure 1), interconnected by flexible strands (*41*). Each of the three SK domains has extensive contact with μPm, which accounts for the strong binding affinity between the two molecules. The crystal structure also suggests that the γ domain may induce a conformational change in Plg resulting in a catalytically competent active site (*41*). Furthermore, the α domain binds near the active site and is thought to provide binding recognition for substrate Plg molecules (*41*). In addition, biochemical evidence has suggested that the N-terminal isoleucine of SK is important in generating an active site in the SK−Plg complex (*42*, *43*). On the basis of sequence homology between the N-terminus of SK and the released N-terminus of the Plg activation bond, it was hypothesized that the N-terminal isoleucine of SK inserts into the activation pocket of Plg to generate a functional active site (*44*).

Since both SK and Plg contain independently folding domains, studies on the interaction of these individual domains during Plg activation may provide insights for the understanding of the activation mechanism. We report here the preparation of recombinant domains from SK and Plg and their roles in binding and activation.

EXPERIMENTAL PROCEDURES

Expression and Purification of Recombinant Proteins. The following recombinant proteins were expressed from pET11 vector (*45*) in *Escherichia coli* strain BL21 (DE3): μPlg_{S741A}, mini-Plg_{S741A}, K5, SK, SKα (SK residues 1−147), SKβ (SK residues 147−290), and SKγ (SK residues 290−414). Both recombinant SK and SKα contain an alanine at position 6 instead of a tryptophan. This residue is located in a disordered region in the crystal structure of SK complexed with μPm (*41*) and should not participate in the interaction. With the exception of K5, all recombinant proteins were expressed as insoluble inclusion bodies that were purified and refolded as described previously (*46*, *47*). Mini-Plg_{S741A} and μPlg_{S741A} were further purified with a Sephacryl S-300 column equilibrated with 20 mM Tris and 0.4 M urea, pH 8.0, followed by a RESOURCE S ion-exchange column (Pharmacia Biotech, Uppsala, Sweden) using a buffer containing 20 mM Hepes and 0.4 M urea, pH 7.0, and eluted with a NaCl gradient from 0.0 to 1.0 M. SK, SKα, SKβ, and SKγ were further purified with a Sephacryl S-300 column equilibrated with 20 mM Tris and 0.4 M urea, pH 8.0, followed by a RESOURCE Q ion-exchange column (Pharmacia Biotech, Uppsala, Sweden) using the same buffer and eluted with a NaCl gradient from 0.0 to 1.0 M.

K5 was purified from *E. coli* as a soluble protein. The bacterial cells were lysed by three passages through a French press in a buffer consisting of 0.1 M Bis-Tris and 1 mM EDTA, pH 6.0, containing one tablet of COMPLETE protease inhibitor cocktail (Boehringer Mannheim). After lysis, 2 mM $MgSO_4$ and 200 mg of DNase were added, and the suspension was stirred until no longer viscous. The lysate was then ultrafiltrated through a membrane with a molecular weight cutoff of 30000. The breakthrough was applied to a G-25 column equilibrated with 20 mM Bis-Tris, pH 6.0. K5 was further purified using a RESOURCE Q ion-exchange column equilibrated with 20 mM Tris, pH 8.5, and eluted with a NaCl gradient from 0.0 to 1.0 M.

Plg_{R561A} was expressed and purified as described previously (*48*). Human Plg was purified from plasma using a variation of the procedure of Deutch and Mertz (*49*, *50*).

Determination of Protein Concentrations. Protein concentrations of samples used in kinetic and binding studies were determined according to the following ϵ_{280} values: 156463 for native full-length human Plg (*2*); 50551 for recombinant μPlg; 67821 for recombinant mini-Plg; 19574 for recombinant kringle 5; 44762 for native SK (*51*); 32588 for recombinant SK; 4868 for recombinant SKα; 11750 for SKβ; and 14960 for recombinant SKγ. The active site concentration of human Plg after activation with SK was determined by the burst titration of Case and Shaw (*52*).

Surface Plasmon Resonance. Association and dissociation between various constructs of SK and Plg were followed in real time by surface plasmon resonance using a BIAcore 1000 biosensor (BIAcore Inc.). In these experiments, full-length SK and its individual domains were separately immobilized onto the surface of a carboxylated dextran matrix (CM-5) sensor chip using the amine coupling kit

provided by the manufacturer. Each immobilization was performed using a 3−5 μg/mL protein solution in 10 mM acetate, pH 4.25, at a flow rate of 5 μL/min. Sequential injections were performed for each ligand until a surface density of 200−400 resonance units (RU) of protein was coupled to the sensor surface. To obtain a control surface for the measurement of the nonspecific refractive index component, a mock coupling was performed using buffer alone. After coupling, the sensor surface was blocked using 1 M ethanolamine, pH 8.5.

Binding experiments were performed in a running buffer containing 10 mM HEPES, pH 7.2, 150 mM NaCl, and 0.005% surfactant P-20, ±10 mM EACA at 25 °C using a flow rate of 30 μL/min. Various concentrations of Plg kringle 5 (0.5−25 μM for all ligands), mini-Plg_{S741A} (20−150 nM for full-length SK ligand), μPlg_{S741A} (20−150 nM for full-length SK ligand, 0.1−1.5 μM for individual SK domain ligands), and native full-length Plg (0.1−2.0 μM for individual SK domain ligands) were separately injected over the sensor surface, and the binding interactions were recorded in the form of sensorgrams. Associations were measured during sample injection (80 s), and then dissociations were measured during injection of running buffer alone (100 s). After each cycle the sensor surface was regenerated by injection of 100 mM Tris buffer, pH 7.2, containing 3.5 M urea.

Unless otherwise stated, and after subtraction of the nonspecific refractive index component, the kinetic constants were calculated from the sensorgrams by nonlinear fitting of the association and dissociation curves according to a 1:1 model A + B = AB using BIAevaluation software version 3.0 (BIAcore, Sweden). The dissociation rate constants (k_{off}) were determined by global fitting of the dissociation data obtained from several analyte concentrations. The association rate constants (k_{on}) were then determined from global fitting of the association data obtained from several analyte concentrations, using the fixed dissociation constants determined previously. Equilibrium dissociation constants (K_d) were then calculated using the relationship $K_d = k_{off}/k_{on}$.

The equilibrium dissociation constants for the binding of kringle 5 to both full-length SK and SKβ were determined from nonlinear curve fitting of the Langmuir binding isotherm to the experimental data (*53*) after subtraction of the nonspecific refractive index component.

One-Stage Plg Activation Assays. The ability of each of the individual domains of SK to activate native full-length Plg was examined using one-stage activation assays. Native full-length Plg (0.25 μM) was separately mixed with each individual domain of SK (0.25−2.5 μM for SKα, 0.25−100 μM for SKβ, and 0.25−5.0 μM for SKγ) and 0.5 mM substrate *N*-*p*-tosyl-Gly-Pro-Lys-*p*NA in a buffer containing 100 mM HEPES, pH 7.4. The generation of amidolytic activity was monitored at 37 °C by measuring the A_{406} for 180 min.

SDS−PAGE Analysis of Plg Activation by SK Domains. Plg (2.5 μM) was mixed individually with each of the domains of SK (25 μM SKα, 100 μM SKβ, and 50 μM SKγ) in a 1 mL volume containing 100 mM HEPES, pH 7.4. At various time intervals (0, 10, 40, and 90 min for SKα; 0, 5, and 20 h for SKβ; 0, 30, 120, and 240 min for SKγ), 50 μL was removed from each reaction and immediately mixed and heated at 100 °C with 50 μL of 2× tricine sample buffer containing 5% β-mercaptoethanol. The samples were electrophoresed on a 10−20% polyacrylamide gradient tricine gel followed by staining with Coomassie blue.

Pm Dependence of Plg Activation by SK Domains. The Pm dependence of Plg activation by the individual domains of SK was examined by varying the amount of Pm at the start of the reaction. The 800 μL activation reactions, all performed in triplicate, contained Plg (0.25 μM), activator (0.25 μM SKα, 2.5 μM SKβ, or 0.25 μM SKγ), and varying concentrations of Pm (0.085−2.5 nM) in a buffer containing 100 mM HEPES, pH 7.4. The reactions were incubated at 37 °C for a duration that was dependent on the activator: 30 min for SKα and 24 h for SKβ and SKγ. The generation of Pm was stopped by the addition of 100 μL of 0.2 mM HEPES, pH 7.4, containing 4 M NaCl. This was followed by the addition of 0.5 mM substrate *N*-*p*-tosyl-Gly-Pro-Lys-*p*NA for a final reaction volume of 1.0 mL. Substrate hydrolysis for each reaction was monitored at 37 °C by measuring the A_{406} for 2 min.

Synergy of Plg Activation. To examine the synergistic behavior between SKα and SKγ, a fixed amount of SKα (0 μM or 0.05 μM) was used to activate 0.5 μM Plg in the presence of varying amounts of SKγ (0−1.5 μM) in an 800 μL reaction containing 100 mM HEPES, pH 7.4. All reactions, performed in triplicate, were incubated at 37 °C for 3 h followed by the addition of 100 μL of buffer containing 4 M NaCl and 200 mM HEPES, pH 7.4, to prevent further activation. This was followed by addition of 0.5 mM substrate *N*-*p*-tosyl-Gly-Pro-Lys-*p*NA for a final reaction volume of 1.0 mL. Substrate hydrolysis for each reaction was monitored at 37 °C by measuring the A_{406} for 5 min.

N-Terminal Methionine Removal from SK and SKα. The N-terminal methionine was removed from SK and SKα using the *E. coli* enzyme methionine aminopeptidase (*54*, *55*). SKΔM and SK$\alpha\Delta$M were then purified using FPLC (as described previously). The extent of removal of the N-terminal methionine was determined by N-terminal sequence analysis.

Active Site Formation Using Plg_{R561A}. Commercial full-length SK (Kabivitrum AB), recombinant SK, SKΔM, SKα, SK$\alpha\Delta$M, SKβ, and SKγ were all tested for the ability to induce an active site in an activation-deficient mutant of full-length Plg containing a mutation at the activation bond (Plg_{R561A}). Full-length SK was tested alone while the individual domains were tested both alone and in combination with each other. In these experiments, 0.25 μM activator(s) was (were) mixed with 0.25 μM Plg_{R561A} and 0.5 mM substrate *N*-*p*-tosyl-Gly-Pro-Lys-*p*NA in a buffer containing 0.1 M HEPES, pH 7.4. Reactions containing SK domains were preincubated at 37 °C for 5 min. Substrate hydrolysis for each 1 mL reaction was monitored at 37 °C by measuring the A_{406} for 25 min.

RESULTS

Binding Interactions between SK and Plg domains. Although the crystal structure of the SK−μPm complex (*41*) had revealed how the SK domains interact with the catalytic unit of Pm, the strengths of these individual interactions, as well as the interactions of the SK domains with the Plg kringles, have not been fully determined. Therefore, we

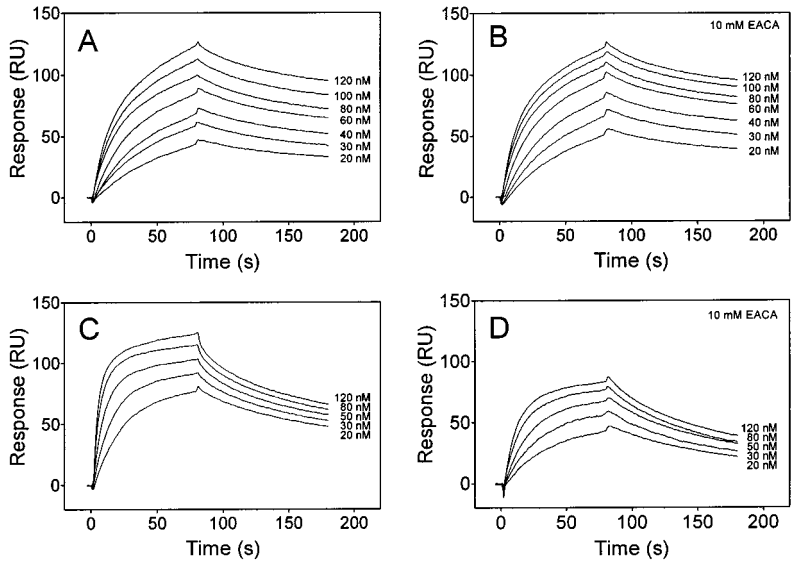

FIGURE 2: Binding interactions between SK and both μPlg_{S741A} and mini-Plg_{S741A}. Overlay plots of different concentrations of μPlg_{S741A} binding to immobilized SK in both the absence (A) and presence (B) of 10 mM EACA. Overlay plots of different concentrations of mini-Plg_{S741A} binding to immobilized SK in both the absence (C) and presence (D) of 10 mM EACA. Sensorgram profiles shown were generated by subtraction of the nonspecific refractive index component from the total binding.

Table 1: Kinetic and Affinity Data for Plg Constructs Binding to SK

analyte	EACA	k_{on} ($\times 10^5$) ($M^{-1}s^{-1}$)	k_{off} ($\times 10^{-3}$) (s^{-1})	K_d ($\times 10^{-9}$) (M)
μPlg_{S741A}	−	4.52 ± 0.04	3.56 ± 0.02	7.88 ± 0.03
mini-Plg_{S741A}	−	19.3 ± 0.12	6.14 ± 0.04	3.18 ± 0.01
K5	−	nd[a]	nd	7130 ± 676
μPlg_{S741A}	+	4.95 ± 0.04	3.39 ± 0.02	6.85 ± 0.01
mini-Plg_{S741A}	+	7.98 ± 0.04	8.44 ± 0.04	10.6 ± 0.01
K5	+	no[b]	no	no

[a] nd indicates not determined. [b] no indicates not observed. Standard error values are based on the global fitting of association and dissociation data.

studied the binding interactions between various domains of SK and Plg employing surface plasmon resonance. For the different Plg constructs used in this study, the active site Ser^{741} was replaced by an alanine to prevent proteolysis during the binding studies. Experiments were performed in the presence of 150 mM NaCl to minimize nonspecific interactions. This had the additional effect of promoting the closed conformation of full-length Plg.

The interactions between immobilized SK and various concentrations of μPlg_{S741A} and mini-Plg_{S741A} were studied in the presence and absence of EACA. Both the sensorgrams (Figure 2) and calculated rate constants (Table 1) indicated that the binding between μPlg_{S741A} and SK is about the same without EACA ($K_d = 7.88$ nM) or with EACA ($K_d = 6.85$ nM). While mini-Plg_{S741A} had a dissociation rate constant almost twice that of μPlg_{S741A}, it had an association rate constant more than 4-fold higher than that of μPlg_{S741A} (Table 1). The resulting 2.5-fold higher affinity of the interaction of SK with mini-Plg_{S741A} apparently comes from the contribution of kringle 5. In addition, EACA increased the K_d between SK and mini-Plg_{S741A} (Table 1) about 3-fold, from 3.18 to 10.6 nM, which was primarily due to the decrease of k_{on} in the presence of EACA, an effect likely mediated by the binding of EACA to kringle 5. These observations suggest that the lysine-binding site in the kringle 5 domain of mini-Plg_{S741A} is involved in binding to SK. Molecular modeling based on the crystal structure of the SK−μPm complex (*41*) suggested that kringle 5 would be in the vicinity for interaction with SK. We therefore measured the binding of kringle 5 to SK. In the absence of EACA, the association and dissociation rates are clearly too fast to be determined (Figure 3A). However, the equilibrium dissociation constant was determined to be 7.13 μM (Table 1) on the basis of the specific RU change at each K5 concentration by nonlinear fitting of the Langmuir binding isotherm to the experimental data (Figure 3B). A Scatchard plot of the data suggested a single class of binding sites (Figure 3B, inset). In contrast, binding between kringle 5 and SK was not observed in the presence of EACA (Table 1), verifying the role of the kringle 5 lysine-binding site.

Similar binding studies were also carried out for immobilized SKα, SKβ, and SKγ with μPlg_{S741A} (sensorgrams not shown). The determined kinetic and affinity data are summarized in Tables 2−4. In the absence of EACA, the K_d values between μPlg_{S741A} and each of the immobilized SK domains were similar, ranging from 65.8 nM for SKα to 87.4 nM for SKγ. These values are approximately an order of magnitude higher than the K_d between μPlg_{S741A} and full-length SK, primarily due to lower association rate constants. EACA had only a moderate effect on the interactions of μPlg_{S741A} with each SK domain (K_d increases: 35% for SKα, 54% for SKβ, and 24% for SKγ). As described above, it is clear that K5 interacts with full-length SK. However, among the individually immobilized SK domains, only K5 interactions with SKβ could be detected. Although the association and dissociation were again too rapid for rate constant calculations (Figure 3C), the equilibrium dissociation constant ($K_d = 5.23$ μM; Table 3) was again computed on the basis of the specific RU change at each K5 concentration (Figure 3D). A Scatchard plot of the data suggested a single class of binding sites (Figure 3D, inset). This affinity was similar to that of K5 toward SK ($K_d = 7.13$ μM) and was also completely abrogated in the presence of EACA (Table 3). These observations indicate that the interaction between

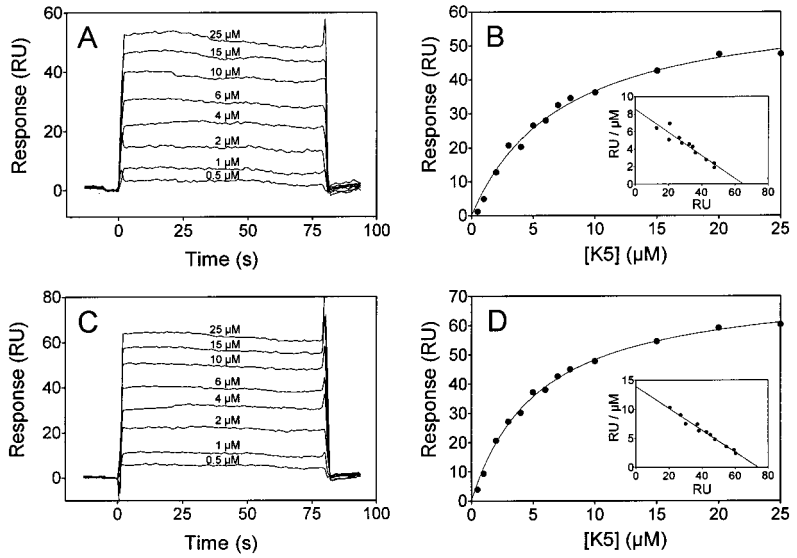

FIGURE 3: Rapid-rate binding interactions. Overlay plots of selected concentrations of K5 binding to both immobilized SK (A) and SKβ (C). The sensorgram profiles shown were generated by subtraction of the nonspecific refractive index component from the total binding. Plots of the specific RU response of varying concentrations of K5 binding to both SK (B) and SKβ (D). K_d values were generated by nonlinear curve fitting of the Langmuir binding isotherm to the experimental data. Scatchard plots of the data are displayed in the insets.

Table 2: Kinetic and Affinity Data for Plg Constructs Binding to SKα

analyte	EACA	k_{on} ($\times 10^5$) ($M^{-1}\,s^{-1}$)	k_{off} ($\times 10^{-3}$) (s^{-1})	K_d ($\times 10^{-9}$) (M)
μPlg$_{S741A}$	−	0.380 ± 0.006	2.50 ± 0.04	65.8 ± 0.1
Plg	−	0.389 ± 0.013	4.47 ± 0.05	115.0 ± 2.6
K5	−	no[a]	no	no
μPlg$_{S741A}$	+	0.400 ± 0.006	3.54 ± 0.03	88.5 ± 0.3
Plg	+	no	no	no
K5	+	no	no	no

[a] no indicates not observed. Standard error values are based on the global fitting of association and dissociation data.

Table 3: Kinetic and Affinity Data for Plg Constructs Binding to SKβ

analyte	EACA	k_{on} ($\times 10^5$) ($M^{-1}\,s^{-1}$)	k_{off} ($\times 10^{-3}$) (s^{-1})	K_d ($\times 10^{-9}$) (M)
μPlg$_{S741A}$	−	0.271 ± 0.010	2.18 ± 0.07	81.0 ± 0.4
Plg	−	0.375 ± 0.019	5.30 ± 0.08	141.0 ± 5.0
K5	−	nd[a]	nd	5230 ± 192
μPlg$_{S741A}$	+	0.319 ± 0.011	3.99 ± 0.09	125.0 ± 1.5
Plg	+	no[b]	no	no
K5	+	no	no	no

[a] nd indicates not determined. [b] no indicates not observed. Standard error values are based on the global fitting of association and dissociation data.

kringle 5 and SK is almost exclusively between the kringle 5 lysine-binding site and the SK β domain.

The binding interactions between full-length Plg and each of the individual domains of SK were evaluated as well (sensorgrams not shown). The kinetic and equilibrium constants are summarized in Tables 2−4. The K_d values for the interactions between Plg and each SK domain were almost twice those of μPlg$_{S741A}$, primarily due to higher k_{off} values. In contrast to μPlg$_{S741A}$, interactions between full-length Plg and each SK domain were not detected in the presence of EACA. Binding interactions between native full-length Plg and full-length SK could not be examined due to rapid Plg activation and subsequent SK degredation.

Table 4: Kinetic and Affinity Data for Plg Constructs Binding to SKγ

analyte	EACA	k_{on} ($\times 10^5$) ($M^{-1}\,s^{-1}$)	k_{off} ($\times 10^{-3}$) (s^{-1})	K_d ($\times 10^{-9}$) (M)
μPlg$_{S741A}$	−	0.374 ± 0.007	3.27 ± 0.03	87.4 ± 0.8
Plg	−	0.389 ± 0.017	5.55 ± 0.11	143.0 ± 3.4
K5	−	no[a]	no	no
μPlg$_{S741A}$	+	0.353 ± 0.008	3.80 ± 0.03	108.0 ± 0.9
Plg	+	no	no	no
K5	+	no	no	no

[a] no indicates not observed. Standard error values are based on the global fitting of association and dissociation data.

Plg Activation by Individual Domains of SK. The ability of the individual domains of SK to activate native full-length Plg was examined using one-stage activation assays. Since preliminary experiments had established that the individual SK domains had low Plg activation activity, reactions were performed in the absence of Cl^- to promote the extended conformation of Plg, thus, increasing assay sensitivity. All three SK domains were found to activate Plg in a concentration-dependent manner (Figure 4A). When used at an equimolar concentration with Plg, the activation ability of SKα was definitive but was only about $^1/_{50000}$ of that of full-length SK (data not shown). The residual activation activities of SKβ and SKγ were confirmed when higher concentrations of these domains were used for Plg activation. SDS−PAGE analysis of the products of Plg activation by each SK domain (Figure 4B) confirmed the generation of both Lys-Plg and Pm. Pm-mediated degradation of the domain activators was also apparent.

Plg Active Site Induction by SK Domains. SK can form an activator complex with either Plg or Pm. In a SK−Plg activator complex, SK induces the catalytic competence of Plg. Therefore, SK can activate Plg in the absence of preformed Pm. However, the study of Plg activation by the SK domains is complicated by the presence of trace amounts of Pm, even in highly purified native Plg preparations. We therefore studied the ability of the individual SK domains to activate Plg in the presence of known initial concentrations

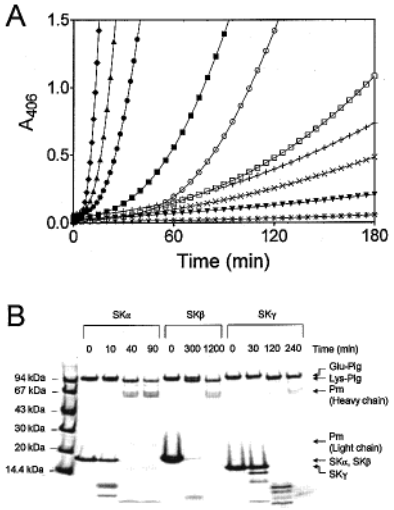

FIGURE 4: Activation of Plg by individual SK domains. (A) Activation of 0.25 μM Plg by 0.25 nM full-length SK (◆), 0.25 μM SKα (■), 1.25 μM SKα (●), 2.5 μM SKα (▲), 0.25 μM SKβ (∗), 50 μM SKβ (×), 100 μM SKβ (+), 0.25 μM SKγ (▼), 1.25 μM SKγ (□), or 5.0 μM SKγ (○) was measured using one-stage activation assays. The generation of amidolytic activity was followed at A_{406} and 37 °C using substrate *N*-*p*-tosyl-Gly-Pro-Lys-*p*NA. (B) SDS−PAGE analysis of mixtures of Plg with each of the individual domains of SK. Plg (2.5 μM) was mixed individually with each of the domains of SK (25 μM SKα, 100 μM SKβ, and 50 μM SKγ). Aliquots were removed at various time intervals.

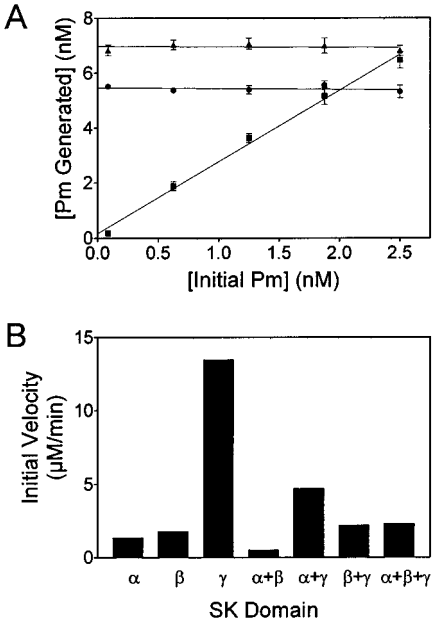

FIGURE 5: Pm dependence of Plg activation and Plg_{R561A} active site formation by SK domains. (A) The activation of 0.25 μM Plg by 0.25 μM SKα (■), 2.5 μM SKβ (●), and 0.25 μM SKγ (▲) was performed in the presence of varying initial concentrations of Pm. The lowest concentration corresponded to the trace level of Pm in the Plg preparation. After activation, Pm was assayed at A_{406} and 37 °C using substrate *N*-*p*-tosyl-Gly-Pro-Lys-*p*NA. The Pm generated by each reaction was calculated by subtracting the initial Pm activity from the final activity. The Pm dependence of each domain was extrapolated to a Pm concentration of zero. Error bars represent the standard deviation between triplicate data points. (B) Ability of the SK domains to induce an active site in Plg_{R561A}. The domains of SK (0.25 μM) were assayed individually and in combination for the ability to generate an active site in 0.25 μM Plg_{R561A}. Amidolytic activity was monitored at A_{406} and 37 °C using substrate *N*-*p*-tosyl-Gly-Pro-Lys-*p*NA. A comparison of each amidolytic activity initial velocity is shown.

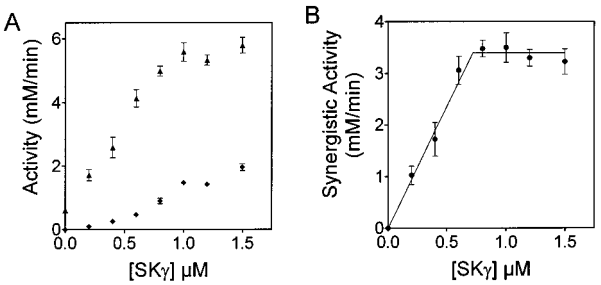

FIGURE 6: Synergy of Plg activation. (A) Varying concentrations of SKγ were used to activate 0.5 μM Plg in the absence (◆) and presence (▲) of 0.05 μM SKα. The Pm generated was assayed at A_{406} and 37 °C using substrate *N*-*p*-tosyl-Gly-Pro-Lys-*p*NA. (B) Synergistic activity was calculated by subtracting the activity generated when each activator was used independently from the activity generated when the activators were used in combination. The solid line represents nominally observed saturation of synergistic activity. Error bars represent the standard deviation between triplicate data points.

of Pm. Figure 5A illustrates that Plg activation by SKβ and SKγ is not dependent, while that of SKα is dependent, on initial Pm concentration. These observations support the contention that SKα provides the activator complex with the function of substrate Plg recognition but lacks the ability to induce active site formation. Conversely, Pm-independent activation suggests that SKγ and, to a lesser extent, SKβ are capable of inducing Plg catalytic activity in the activator complex.

To further substantiate these observations, the domains of SK were tested for the ability to induce an active site in Plg_{R561A}. This full-length Plg mutant contains an uncleavable activation bond and, thus, cannot be activated into Pm. However, full-length SK can still bind and create a competent active site within Plg_{R561A} (*48*). When used individually at an equimolar concentration with Plg_{R561A}, significant active site induction was observed with SKγ, while only residual active site formation was detected with either SKα or SKβ (Figure 5B). These observations confirmed the results of the Pm dependence of Plg activation studies, suggesting that SKγ can induce the formation of an active site in Plg. The residual active site induction by SKα further suggests that its primary role is to provide the activator complex with the specificity to bind substrate Plg. In addition to its extremely low Plg activation activity, SKβ exhibits only a very poor ability to induce an active site in Plg_{R561A}.

Synergy by SK Domains. The ability of the different domains of SK to act synergistically was examined by combining SK domains in Plg activation assays. These experiments measured the Plg activation levels of domain combinations beyond the additive amounts of the domains alone. Among the combinations of domains, only SKα with SKγ had a synergistic effect, which increased with increasing concentrations of SKγ added to a constant amount of SKα (Figure 6). At the maximum, the synergistic activity was about 4 times the combined activities of the two domains measured alone (data not shown). These results are consistent with the idea that SKα and SKγ perform different functions in the mechanism of SK-mediated Plg activation.

The effect of combining SK domains on Plg_{R561A} active site formation was also examined. However, combining domains consistently produced lower activity than that of the highest individual domain component (Figure 5B). The

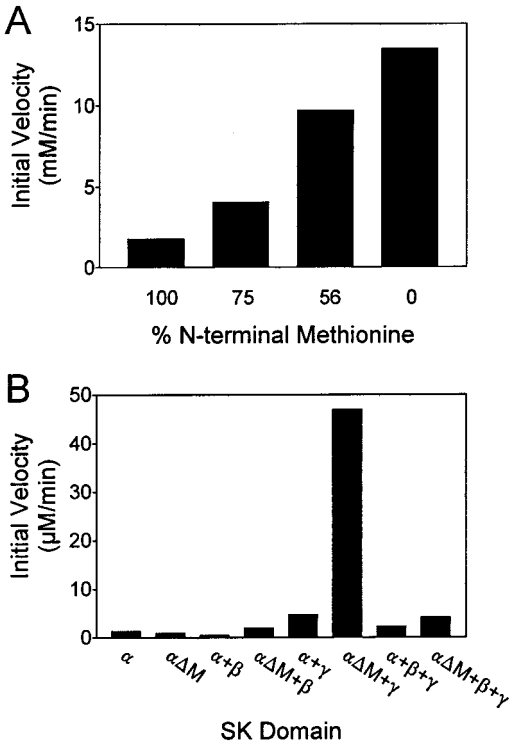

FIGURE 7: Effect of the SK and SKα N-terminus on Plg_{R561A} active site formation. (A) SK (0.25 μM) containing varying percentages of N-terminal methionine was assayed for the ability to generate an active site in 0.25 μM Plg_{R561A}. Amidolytic activity was monitored at A_{406} and 37 °C using substrate *N*-*p*-tosyl-Gly-Pro-Lys-*p*NA. (B) Effect of SKα N-terminal methionine removal on its ability to induce an active site in Plg_{R561A} when in combination with other SK domains. SKα (0.25 μM) and SKαΔM with 30% of the N-terminal methionine removed (0.25 μM) were assayed alone and in combination with the other SK domains (0.25 μM each) for the ability to induce an active site in 0.25 μM Plg_{R561A}. Amidolytic activity was monitored at A_{406} and 37 °C using substrate *N*-*p*-tosyl-Gly-Pro-Lys-*p*NA. A comparison of each amidolytic activity initial velocity is shown.

reason for the antagonism among the domains is not clear. Perhaps interactions between domains interfere with their interactions with Plg_{R561A}.

Effect of the SK N-Terminal Residue on Plg Activation. The N-terminal residue of SK has been shown to be important for the induction of an active site in Plg (*42*). The fact that recombinant SK, expressed in *E. coli*, contained an extra methionine beyond the native N-terminal Ile^1 provided a system to study its importance. Methionine aminopeptidase was used to partially remove the N-terminal methionine residue from SK, and the subsequent effect on Plg_{R561A} active site formation was measured. Native SK (Kabivitrum AB) with an N-terminal Ile^1 is about 7 times more active than SK containing an N-terminal methionine (Figure 7A). Samples of SK containing 75% and 56% N-terminal methionine had activity increases closely proportional to the amount of methionine removed (Figure 7A). These results indicate that the N-terminal Ile^1 strongly enhanced, but is not necessary for, the ability of full-length SK to induce an active site in Plg_{R561A}.

N-Terminal sequence analysis of each of the SK domains (data not shown) revealed that recombinant SKα, but not SKβ or SKγ, had an extra methionine at the N-terminus from its heterologous expression in *E. coli*. This provided an opportunity to examine the effect of the SKα N-terminus on Plg_{R561A} active site formation. Although we were only able to remove 30% of the N-terminal methionine from SKα (SKαΔM), some differences in active site inducing ability could clearly be detected. While the activity of SKαΔM was not higher than that of SKα, the activity of SKαΔM + SKγ was considerably higher than that of SKα + SKγ (Figure 7B). Also, while SKα appeared to inhibit the activity of SKγ (Figure 5B), SKαΔM increased the activity by 3.5-fold (Figures 5B and 7B). However, it should be noted that, in the mixture of all three domains, the partial removal of the N-terminal methionine from SKα did not overcome the quenching effect from the addition of SKβ. These data suggest that the native N-terminal Ile^1 on SKα can cooperatively enhance the induction of an active site in Plg_{R561A} by SKγ.

DISCUSSION

The first step in SK-mediated Plg activation is the formation of a SK−Plg complex, with a K_d estimated to be in the range of 0.22 μM to 28 pM (*56*−*62*). We report here K_d values of 7.88 and 3.18 nM for full-length SK binding to μPlg_{S741A} and mini-Plg_{S741A}, respectively. A previous study, also using surface plasmon resonance, reported a K_d of 28 pM for SK binding to full-length Plg (*61*). However, this higher affinity is similar to K_d values recently reported for SK binding to Pm (11−19 pM) (*24*, *63*), suggesting that the presence of Pm may have been responsible for the K_d value in the picomolar range. It is important to note that both recombinant SK and SKα, expressed in *E. coli*, contain an extra methionine beyond the native N-terminal Ile^1. However, it has been demonstrated that Ile^1 does not contribute to the affinity of SK for Plg (*43*).

The three domains of SK bind to the catalytic unit of Plg (μPlg_{S741A}) with similar strength: K_d values of 65.8, 81.0, and 87.4 nM for domains α, β, and γ, respectively (Tables 2−4). This similarity is in agreement with the crystal structure of the SK−μPm complex, which illustrates that the interacting surfaces of the three SK domains with μPm are similar in size (*41*). Various evidence from these studies supports the idea that each of the individual SK domains binds to a specific region of μPlg_{S741A}, most likely in a manner comparable to that of the SK−μPm complex. First, the binding data fit a 1:1 model. Second, different properties are observed for the different SK domains. The Pm dependence of Plg activation (Figure 5A), Plg active site formation (Figures 5B and 7B), and the synergy of Plg activation (Figure 6) all show clear domain specificity, which could not have resulted from nonspecific binding of the domains. Finally, although the SK domains are structurally homologous, their sequences and surface residues are drastically different. A comparison on the interacting surfaces of the three domains suggests that they cannot significantly cross-bind to Plg (data not shown). We note that the K_d for the SK-μPlg_{S741A} interaction (7.88 nM) is only about 10-fold lower than the values determined with each of the individual SK domains. While this value is higher than would be predicted from the combined interaction of three independent binding sites, it may be the result of stepwise interactions in an interdependent multidomain system.

The K_d values for full-length Plg binding to SKα, SKβ, and SKγ are near, but higher, than those for μPlg binding

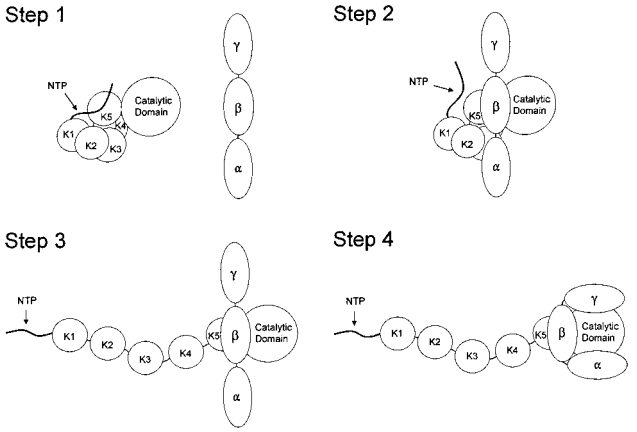

FIGURE 8: Model of SK binding to Plg. The individual domains are labeled. Step 1: Noninteracting Plg and SK. Plg is in the closed conformation. Step 2: The SK β domain binds to Plg kringle 5, displacing the Plg NTP. Step 3: Plg is converted from the closed to the extended conformation. Step 4: All three domains of SK bind to the catalytic domain of Plg.

to the corresponding SK domains. Interestingly, the higher Plg values are caused by a higher k_{off} for all three SK domains (Tables 2−4), suggesting that the presence of the NTP and kringles results in a less stable complex between the catalytic unit of Plg and an independent domain of SK. A wide range of binding affinities of Plg to a region of SK similar to SKβ have been reported in the literature, from 3.33 to 400 nM (*56*, *58*, *60*, *61*). The K_d reported here (141.0 nM) falls near the middle of the range. Current data also demonstrate that kringle 5 binds to SKβ with a K_d of about 5.2 μM (Table 3). The interaction of SKβ with kringle 5 had been predicted by molecular modeling of the SK−Plg interaction (*41*). Interaction of kringle 5 with either SKα or SKγ was not detected and is probably insignificant since the K_d of the interaction of kringle 5 with full-length SK is 7.13 μM (Table 1), a value very near to that of the interaction between kringle 5 and SKβ. The fact that the kringle 5 interaction with SKβ is abolished by EACA (Table 3) suggests that the binding is mediated by the lysine-binding site of kringle 5 and a lysine side chain in SKβ. In agreement with previously reported results using surface plasmon resonance (*61*), binding of SKβ to full-length Plg is also abolished by EACA (Table 3). This is in contrast to the interaction between SKβ and μPlg$_{S741A}$, which is only slightly affected by EACA (Table 3). These observations support recent evidence that activator complex formation with full-length Plg occurs through a kringle-dependent mechanism (*62*). The most plausible explanation is that binding between kringle 5 and the SKβ domain is the initial and obligatory step in the interaction between SK and full-length Plg. This is supported by the observations presented here that SKβ binds to K5 far more rapidly than it binds the Plg catalytic domain. Recent evidence that SK has a significantly higher affinity toward the extended conformation of Plg, through interactions involving lysine-binding sites, suggested a model in which the closed form of Plg changes conformation upon binding to SK (*24*). On the basis of the current evidence, a model for the formation of a SK−Plg complex is proposed here (Figure 8). In free Plg (Figure 8, step 1), a lysine located in the NTP domain is bound to kringle 5 (*64*, *65*). When SK is present, a lysine in the β domain rapidly replaces the NTP for kringle 5 binding [Figure 8, steps 2 and 3, suggested by Conejero-Lara et al. (*61*)]. This low-affinity obligatory step leads to the conversion of Plg from the closed to the extended conformation and is followed by tight binding of all three SK domains to the catalytic unit of Plg (Figure 8, step 4), similar to the structure of the SK−μPm complex (*41*).

Current results also provide insight into the functions of individual SK domains during Plg activation. SK has the unique ability to induce, without peptide bond cleavage, a catalytically competent active site in the Plg moiety of the activator complex. The structural basis for this active site induction has been proposed, on the basis of the crystal structure of the SK−μPm complex, by Wang et al. (*41*). In this model, the binding of SKγ to the "autolysis loop" region of Plg, residues 692−695, near the activation cleavage site, causes a conformational change resulting in the formation of a new salt linkage, possibly between Lys^{698} and Asp^{740}, leading to active site formation. An equivalent salt linkage is known to exist in the catalytically active zymogen form of tissue plasminogen activator (*66*−*68*). Modeling based on the structures of μPlg and the SK−μPm complex revealed that Lys^{698} can be repositioned to form the critical salt linkage (*41*). A second hypothesis suggests that, in the SK−Plg complex, the N-terminal Ile^1 of SK inserts into the activation pocket of Plg and forms the crucial salt bridge with Plg Asp^{740}, thus inducing the active conformation of Plg (*42*, *44*, *69*). Recently, it was shown that mutation of Lys^{698} in μPlg$_{R561A}$ decreased its binding affinity toward SK, which in turn reduced the level of active site induction (*43*). The exact contribution of Plg Lys^{698} to SK-mediated active site induction remains unclear. The same report also demonstrated that mutation of SK Ile^1 reduced its ability to induce an active site in μPlg$_{R561A}$ (*43*), supporting previous results obtained by the deletion of SK Ile^1 (*42*). These results are consistent with the N-terminal insertion hypothesis; however, the possibility that SK Ile^1 functions to stabilize a Plg active site induced by another mechanism cannot be excluded. These results, in addition to the results presented here, clearly demonstrate the importance of SK N-terminal residue Ile^1.

The current results indicate that SKγ, and to a much lesser extent SKβ, can independently induce active site formation in Plg. Although all three SK domains can activate native Plg (Figure 4A), the activity of SKα is Pm dependent (Figure 5A); thus its contribution to Plg activation lies in the recognition of substrate Plg rather than the induction of a Plg active site. The activity of SKβ is very low (Figure 4A) but appears to be Pm independent (Figure 5A). The active site inducing ability of SKγ is clearly substantiated from the use of Plg$_{R561A}$, which has a mutated activation bond; thus, amidolytic activity can only be generated by binding induction of an active site (*48*). This role of SKγ is in agreement with a recently published report indicating that the coiled-coil region of the SK γ domain is essential for induction of an active site within the Plg moiety of the activator complex (*70*). While SKγ induced a measurable active site in Plg$_{R561A}$, the other two SK domains had only residual activities (Figure 5B). Whether these residual activities represent their roles in the full-length SK molecule remains to be shown. As already mentioned, SKα has an extra methionine at the N-terminus, but removal of this methionine did not improve its ability to induce an active site in Plg$_{R561A}$ (Figure 7B). Although SKα cannot independently induce significant active site formation in Plg$_{R561A}$, it renders the ability of the activator

complex to recognize substrate Plg, as shown by its Pm dependence of Plg activation (Figure 5A). Therefore, the mechanism of Plg activation by individual SKα is analogous to that of staphylokinase, which not only is structurally homologous to SKα (*71*) but also requires the presence of Pm for Plg activation (*48*). The contribution of staphylokinase to the recognition of substrate Plg is established from the crystal structure (*71*), which bears much resemblance with the structural relationship of the SK α domain in the SK−μPm complex (*41*). Taken together, all of the evidence supports the contention that substrate recognition is the primary function of the SK α domain.

The N-terminal Ile^1 of SKα is apparently important for amplifying the ability of SKγ to induce a functional active site in Plg_{R561A} (Figure 7B). This same effect is likely also responsible for the increase of activity when the extra N-terminal methionine is removed from recombinant full-length SK (Figure 7A). Although these results are compatible with the physical model of the SK N-terminal insertion hypothesis (*42*, *44*, *69*), the major discrepancy, however, lies with the observation that SKα with the N-terminal Ile^1 did not significantly induce a functional active site in Plg_{R561A}. Since SKα can bind tightly to Plg, active site formation in the zymogen would be predicted by the insertion hypothesis. The importance of Ile^1 to the overall activity of SK has been well demonstrated (*42*, *43*). However, the current results suggest that the role of SK Ile^1 is the augmentation and stabilization of the new Plg conformation induced by the SK γ domain, which does not necessarily involve its insertion into the Plg activation pocket. Furthermore, static molecular modeling suggests that N-terminal insertion is unlikely to be responsible for the activity of recombinant SK with an N-terminal methionine. The Met^1 side chain is too large to be accommodated by the Plg activation pocket, and such an insertion would disrupt the geometry of the all-important salt linkage between the α-amino group of SK Met^1 and the carboxyl group of Plg Asp^{740}. From these analyses, the ability of recombinant SK to generate amidolytic activity in Plg_{R561A} suggests that N-terminal insertion is not required for the active site generating ability of SK.

In summary, the present study further defines the functional roles of the three domains of SK during Plg activation. In the case of free Plg, SK−Plg complex formation is initiated by the rapid and obligatory interaction between the SK β domain and Plg kringle 5. This interaction triggers the conversion of Plg from the closed to the extended conformation and is followed by binding of all three SK domains to the catalytic domain of Plg. Active site formation in the Plg moiety of the activator complex is cooperatively induced by both the SK α and γ domains, while substrate Plg is recognized by the activator complex through interactions predominately mediated by the SK α domain.

ACKNOWLEDGMENT

The authors thank Dr. Pierre Neuenschwander for helpful discussions about BIAcore experiments, Dr. Gerald Koelsch for assistance with manuscript preparation, and both Dr. W. Todd Lowther and Dr. Brian W. Matthews for the generous gift of methionine aminopeptidase. Amino acid analysis and N-terminal sequencing were performed by the Molecular Biology Resource Facility, Warren Medical Research Institute, University of Oklahoma Health Sciences Center. Jordan Tang is holder of the J. G. Puterbaugh Chair in Biomedical Research at the Oklahoma Medical Research Foundation.

REFERENCES

1. Sottrup-Jensen, L., Claeys, H., Zajdel, M., Petersen, T. E., and Magnusson, S. (1978) *Prog. Chem. Fibrinolysis Thrombolysis 3*, 191−209.
2. Violand, B. N., and Castellino, F. J. (1976) *J. Biol. Chem. 251*, 3906−3912.
3. Castellino, F. J., Ploplis, V. A., Powell, J. R., and Strickland, D. K. (1981) *J. Biol. Chem. 256*, 4778−4782.
4. Lerch, P. G., Rickli, E. E., Lergier, W., and Gillessen, D. (1980) *Eur. J. Biochem. 107*, 7−13.
5. Castellino, F. J., and Powell, J. R. (1981) *Methods Enzymol. 80*, 365−378.
6. Motta, A., Laursen, R. A., Llinas, M., Tulinsky, A., and Park, C. H. (1987) *Biochemistry 26*, 3827−3836.
7. Sehl, L. C., and Castellino, F. J. (1990) *J. Biol. Chem. 265*, 5482−5486.
8. Thewes, T., Constanine, K., Byeon, I. J., and Llinas, M. (1990) *J. Biol. Chem. 265*, 3906−3915.
9. Menhart, N., Sehl, L. C., Kelley, R. F., and Castellino, F. J. (1991) *Biochemistry 30*, 1948−1957.
10. Wiman, B., and Wallen, P. (1977) *Thromb. Res. 10*, 213−222.
11. Wiman, B., Lijnen, H. R., and Collen, D. (1979) *Biochim. Biophys. Acta 579*, 142−154.
12. Lucas, M. A., Fretto, L. J., and McKee, P. A. (1983) *J. Biol. Chem. 258*, 4249−4256.
13. Wu, H. L., Chang, B. I., Wu, D. H., Chang, L. C., Gong, C. C., Lou, K. L., and Shi, G. Y. (1990) *J. Biol. Chem. 265*, 19658−19664.
14. Alkjaersig, N., Fletcher, A. P., and Sherry, S. (1959) *J. Biol. Chem. 234*, 832−837.
15. Abiko, Y., Iwamoto, M., and Tomikawa, M. (1969) *Biochim. Biophys. Acta 185*, 424−431.
16. Shi, G. Y., and Wu, H. L. (1988) *J. Biol. Chem. 263*, 17071−17075.
17. Christensen, U., Sottrup-Jensen, L., Magnusson, S., Petersen, T. E., and Clemmensen, I. (1979) *Biochim. Biophys. Acta 567*, 472−481.
18. Shi, G. Y., Change, B. I., Wu, D. H., Ha, Y. M., and Wu, H. L. (1990) *Thromb. Res. 58*, 317−329.
19. Tranqui, L., Prandini, M. H., and Chapel, A. (1979) *Biol. Cell. 34*, 39−42.
20. Ponting, C. P., Holland, S. K., Cederholm-Williams, S. A., Marshall, J. M., Brown, A. J., Spraggon, G., and Blake, C. F. (1992) *Biochim. Biophys. Acta 1159*, 155−161.
21. Weisel, J. W., Nagaswami, C., Korsholm, B., Petersen, L. C., and Suenson, E. (1994) *J. Mol. Biol. 235*, 1117−1135.
22. Urano, T., Chibber, B. A., and Castellino, F. J. (1987) *Proc. Natl. Acad. Sci. U.S.A. 84*, 4031−4034.
23. McCance, S. G., and Castellino, F. J. (1995) *Biochemistry 34*, 9581−9586.
24. Boxrud, P. D., and Bock, P. E. (2000) *Biochemistry 39*, 13974−13981.
25. Ponting, C. P., Marshall, J. M., and Cederholm-Williams, S. A. (1992) *Blood Coag. Fibrinolysis 3*, 605−614.
26. Horrevoets, A. J., Smilde, A. E., Fredenburgh, J. C., Pannekoek, H., and Nesheim, M. E. (1995) *J. Biol. Chem. 270*, 15770−15776.
27. Castellino, F. J., Brockway, W. J., Thomas, J. K., Liano, H. T., and Rawitch, A. B. (1973) *Biochemistry 12*, 2787−2791.
28. Sjoholm, I. (1973) *Eur. J. Biochem. 39*, 471−479.
29. Violand, B. N., Byrne, R., and Castellino, F. J. (1978) *J. Biol. Chem. 253*, 5395−5401.
30. Mangel, W. F., Lin, B. H., and Ramakrishnan, V. (1990) *Science 248*, 69−73.
31. Christensen, U., and Molgaard, L. (1992) *Biochem. J. 285*, 419−425.

32. Freer, S. T., Kraut, J., Robertus, J. D., Wright, H. T., and Xuong, N. H. (1970) *Biochemistry 9*, 1997−2009.
33. Reddy, K. N., and Markus, G. (1972) *J. Biol. Chem. 247*, 1683−1691.
34. Schick, L. A., and Castellino, F. J. (1974) *Biochem. Biophys. Res. Commun. 57*, 47−54.
35. Summaria, L., and Robbins, K. C. (1976) *J. Biol. Chem. 251*, 5810−5813.
36. Castellino, F. J. (1979) *Trends Biochem. Sci. 4*, 1−5.
37. McClintock, D. K., and Bell, P. H. (1971) *Biochem. Biophys. Res. Commun. 43*, 694−702.
38. Reddy, K. N., and Markus, G. (1974) *J. Biol. Chem. 249*, 4851−4857.
39. Reddy, K. N. (1988) *Enzyme 40*, 79−89.
40. Gonzalez-Gronow, M., Siefring, G. E., Jr., and Castellino, F. J. (1978) *J. Biol. Chem. 253*, 1090−1094.
41. Wang, X., Lin, X., Loy, J. A., Tang, J., and Zhang, X. C. (1998) *Science 281*, 1662−1665.
42. Wang, S., Reed, G. L., and Hedstrom, L. (1999) *Biochemistry 38*, 5232−5240.
43. Wang, S., Reed, G. L., and Hedstrom, L. (2000) *Eur. J. Biochem. 267*, 3994−4001.
44. Jackson, K. W., and Tang, J. (1978) *Thromb. Res. 13*, 693−699.
45. Studier, F. W., Rosenberg, A. H., Dunn, J. J., and Dubendorff, J. W. (1990) *Methods Enzymol. 185*, 60−89.
46. Lin, X. L., Wong, R. N., and Tang, J. (1989) *J. Biol. Chem. 264*, 4482−4489.
47. Lin, X. L., Lin, Y. Z., and Tang, J. (1994) *Methods Enzymol. 241*, 195−224.
48. Grella, D. K., and Castellino, F. J. (1997) *Blood 89*, 1585−1589.
49. Deutsch, D. G., and Mertz, E. T. (1970) *Science 170*, 1095−1096.
50. Bennett, W. F., Paoni, N. F., Keyt, B. A., Botstein, D., Jones, A. J., Presta, L., Wurm, F. M., and Zoller, M. J. (1991) *J. Biol. Chem. 266*, 5191−5201.
51. Taylor, F. B., Jr., and Botts, J. (1968) *Biochemistry 7*, 232−242.
52. Chase, T., Jr., and Shaw, E. (1969) *Biochemistry 8*, 2212−2224.
53. Mehta, P., Cummings, R. D., and McEver, R. P. (1998) *J. Biol. Chem. 273*, 32506−32513.
54. Lowther, W. T., McMillen, D. A., Orville, A. M., and Matthews, B. W. (1998) *Proc. Natl. Acad. Sci. U.S.A. 95*, 12153−12157.
55. Lowther, W. T., and Matthews, B. W. (2000) *Biochim. Biophys. Acta 1477*, 157−167.
56. Rodriguez, P., Fuentes, P., Barro, M., Alvarez, J. G., Munoz, E., Collen, D., and Lijnen, H. R. (1995) *Eur. J. Biochem. 229*, 83−90.
57. Reed, G. L., Lin, L. F., Parhami-Seren, B., and Kussie, P. (1995) *Biochemistry 34*, 10266−10271.
58. Nihalani, D., and Sahni, G. (1995) *Biochem. Biophys. Res. Commun. 217*, 1245−1254.
59. Bock, P. E., Day, D. E., Verhamme, I. M., Bernardo, M. M., Olson, S. T., and Shore, J. D. (1996) *J. Biol. Chem. 271*, 1072−1080.
60. Nihalani, D., Raghava, G. P., and Sahni, G. (1997) *Protein Sci. 6*, 1284−1292.
61. Conejero-Lara, F., Parrado, J., Azuaga, A. I., Dobson, C. M., and Ponting, C. P. (1998) *Protein Sci. 7*, 2190−2199.
62. Lin, L. F., Houng, A., and Reed, G. L. (2000) *Biochemistry 39*, 4740−4745.
63. Boxrud, P. D., Fay, W. P., and Bock, P. E. (2000) *J. Biol. Chem. 275*, 14579−14589.
64. Marshall, J. M., Brown, A. J., and Ponting, C. P. (1994) *Biochemistry 33*, 3599−3606.
65. Cockell, C. S., Marshall, J. M., Dawson, K. M., Cederholm-Williams, S. A., and Ponting, C. P. (1998) *Biochem. J. 333*, 99−105.
66. Tachias, K., and Madison, E. L. (1997) *J. Biol. Chem. 272*, 28−31.
67. Renatus, M., Engh, R. A., Stubbs, M. T., Huber, R., Fischer, S., Kohnert, U., and Bode, W. (1997) *EMBO J. 16*, 4797−4805.
68. Bode, W., and Renatus, M. (1997) *Curr. Opin. Struct. Biol. 7*, 865−872.
69. Bode, W., and Huber, R. (1976) *FEBS Lett. 68*, 231−236.
70. Wu, D. H., Shi, G. Y., Chuang, W. J., Hsu, J. M., Young, K. C., Chang, C. W., and Wu, H. L. (2001) *J. Biol. Chem. 276*, 15025−15033.
71. Parry, M. A. A., Fernandez-Ctalan, C., Bergner, A., Huber, R., Hopfner, K., Schlott, B., Guhrs, K., and Bode, W. (1998) *Nat. Struct. Biol. 5*, 917−923.

BI011309D